Guidance, Control, and Dynamics
Vol. 1, No. 1, December 2003

Numerical Single-Degree-of-Freedom Analysis and Control of an 80 Degree Delta Wing with an Analytical Roll Moment Model

Charles R. O'Neill*
Oklahoma State University, Stillwater, Oklahoma 74078

This project surveys nonlinear analysis and control methods for a specific two-degree-of-freedom analytical delta wing model. Linearization, phase plane analysis and existence theorems are used to describe the overall system behavior without solving the differential equations. A describing function is developed for the nonlinear system and favorably compares to the actual limit cycle amplitudes and frequencies. Linear pole placement and Ricatti control methods and nonlinear sliding mode and Lyapunov control laws are developed for stabilization and tracking.

Nomenclature

L	Roll Moment
C_L	Roll Moment Coefficient (L/Q)
Q	Moment Non-Dimensionalization
θ	Pitch Angle
p	Roll Rate
q	Pitch Rate
r	Yaw Rate
α	Angle of Attack
β	Sideslip Angle
b	Wing Span
c	Chord Length
$I_{\hat{v}}$	Body Axis Moment Of Inertia

Introduction

Delta wing at high pitch angles exhibit nonlinear roll behavior. The nonlinear behavior comes from nonlinear aerodynamics resulting from axial vortical flow. The typical symptom found by an aircraft designer is wing rock, an undesirable limit cycle in roll.

This project numerically analyzes a two degree of freedom delta wing model. Aircraft equations of motion are reviewed to compare the selected model with actual physics and aerodynamics. The objective is to select an analytical governing equation for the rolling motion and analyze the model with tools available in the phase plane. A control section will evaluate linear and nonlinear control schemes for roll stabilization and tracking.

Aircraft Equations of Motion

The governing aircraft equations of motion are Newton's Second Law in a body fixed reference frame.[1] Adding the body fixed reference frame frees the analysis from time-varying body properties at the expense of nonlinear equations of motion. Conversion between the body fixed and inertia reference frame is through Euler angles —three order-dependent successive rotations. For this paper, only the roll degree of freedom is considered. The general aircraft equation of motion in the roll axis is:[1]

$$I_x\dot{p} - I_{xz}\dot{r} + (I_z - I_y)qr - I_{xy}pq = L$$

The yaw and pitch rates are fixed at zero. Substituting the Euler roll angle, $\dot{\Phi} = p$, yields a single second order differential equation for roll angle.

$$I_x\ddot{\Phi} = L \tag{1}$$

The aerodynamics enter the motion through the moment L. L is a complicated function of the body fixed orientation with respect to the freestream velocity vector. For a general derivation, the Euler Angles are converted into the body fixed reference frame. The body fixed velocity vector orientation with respect to the Euler orientation angles is:

$$\begin{aligned} \alpha &= \text{atan}(\tan\theta_0 \cos\phi) \\ \beta &= \text{asin}(\sin\theta_0 \sin\phi) \\ \dot{\beta} &= \dot{\phi}(\sin\theta_0 \sin\phi)/\sqrt{1 - \sin^2\theta\cos^2\phi} \end{aligned}$$

Knowing the freestream velocity vector allows for computing the roll moment L while preserving the body fixed reference frame.

Delta Wing Aerodynamics

Delta wing aerodynamics at high angles of attack are primarily dominated by axial vortices emanating off the leading edge. Experiments[2] and theoretical reviews[3] explain some of the aerodynamic mechanisms responsible for the nonlinear behavior.

General Aerodynamic Model

A general aerodynamic model is complicated. Conceptually, the aerodynamic roll moment depends on the freestream velocity vector in the body fixed frame. The conceptual roll moment is probably of the form:

$$L/Q = C_L = f(\alpha, \beta)$$

Any physically consistent model will need these terms. From the previous section, it is seen that the relationship between the freestream orientation and the Euler angles is complicated. Incompressible aerodynamic theory predicts that aerodynamic forces result from motion terms up to acceleration, so the Euler angle relationships up to acceleration will be required.

Selected Aerodynamic Model

The difficulties of state space modeling becomes finding an appropriate roll moment function. Because the focus of this project is to survey many nonlinear analysis techniques, an analytical roll moment function is desired. The specific roll moment model used for this paper is from Nayfeh, Elzebda and Mook.[4] The aerodynamic model was developed by fitting unsteady aerodynamic data to a function of the form:

$$C_L = a_1\phi + a_2\dot{\phi} + a_3\phi^3 + a_4\phi^2\dot{\phi} + a_5\phi\dot{\phi}^2 \tag{2}$$

Nayfeh, Elzebda and Mook.[4] claim "virtually perfect agreement" between the model and the actual aerodynamic data. No limitations on motion inputs were reported. From their paper, the model appears tuned to motion *inside* the limit cycles. The model is defined with tabulated coefficients for four angles of attack. These coefficients are tabulated in Table 1.

In hindsight, the limitations and over-simplification of this model is evident. In particular, this model is not harmonic with roll angle as physics demands. However, finding an analytic model with pleasant properties is difficult. This particular model was selected as the best among several alternative models —one alternative was especially tempting.[5]

*Graduate Research Assistant, Student Member AIAA
Submitted as a Final Project in MAE 5463 Nonlinear System Analysis and Control on Dec. 4, 2003.

Table 1 Model Coefficients for Eq. (2)

θ	a_1	a_2	a_3	a_4	a_5
15.0	-0.01026	-0.02117	-0.14181	0.99735	-0.83478
21.5	-0.04207	0.01456	0.04714	-0.18583	0.24234
22.5	-0.04681	0.01966	0.05671	-0.22691	0.59065
25.0	-0.05686	0.03254	0.07334	-0.35970	1.46810

State Space Model

Combining the aircraft equations of motion with the aerodynamic roll moment model produces a governing equation for the delta wing's rolling motion Eq. (3).

$$\ddot{\phi}/Q = a_1\phi + a_2\dot{\phi} + a_3\phi^3 + a_4\phi^2\dot{\phi} + a_5\phi\dot{\phi}^2 \tag{3}$$

The state space representation is:

$$\begin{aligned} \dot{x}_1 &= x_2 \\ \dot{x}_2 &= Q\left(a_1x_1 + a_2x_2 + a_3x_1^3 + a_4x_1^2x_2 + a_5x_1x_2^2\right) \end{aligned} \tag{4}$$

The roll moment non-dimensionalization parameter Q is taken as 0.354 as given by Nayfeh, Elzebda and Mook.[4] Incidentally, time is scaled by $t^* = U_0/L_0 t$. For this particular model the non-dimensionalization constant is approximately 140. So 140 seconds of non-dimensional time is approximately 1 actual second.

Equilibrium Points and Nullclines

Analysis of equilibrium points and nullclines provide insights into the solutions of differential equations without requiring trajectory solutions.

Equilibrium points

Equilibrium points are where the system response is unchanging. This occurs when the state vector is zero. Solving the first state equation for a zero state vector yields:

$$\dot{x}_1 = 0 = x_2$$

So, all equilibrium points lie on the x axis ($x_2 = 0$). Substituting into the second state equation yields:

$$\dot{x}_2 = 0 = +a_1x_1 + a_3x_1^3 + f(x_2)$$

Solving shows either $x_1 = 0$ or $x_1 = \pm\sqrt{-a_1/a_3}$. For this particular delta wing model, three equilibrium points are possible. The equilibrium points are:

$$\begin{aligned} x_1 &= \{0, \pm\sqrt{-a_1/a_3}\} \\ x_2 &= 0 \end{aligned}$$

At 25 degrees, the equilibrium points are at $x_2 = 0$ with $x_1 = 0$ and $x_1 \approx \pm 0.88$. Only the origin is an equilibrium point at 15 degrees pitch angle.

Nullclines

Nullclines are the set of locations where the solution trajectories directions are either horizontal or vertical. A nullcline is the set of all points where one state equation is zero.

The vertical nullcline occurs when $\dot{x}_1 = 0$. For this particular model, the vertical nullcline exists when:

$$x_2 = 0$$

The horizontal nullcline occurs when $\dot{x}_2 = 0$. Solving the second state space equation in Eq. (5) for x_2 yields:

$$x_2 = \frac{-a_2 - a_4\,x_1^2}{2a_5\,x_1} \pm \frac{\sqrt{a_2^2 + 2\,a_2\,a_4\,x_1^2 + a_4^2 x_1^4 - 4\,a_5\,x_1^2 a_1 - 4\,a_5\,x_1^4 a_3}}{2a_5\,x_1}$$

The vertical and horizontal nullclines are plotted in the phase plane in Figs. 1 and2 for four pitch angles. The nullclines for $\theta = \{21.5 - 25^\circ\}$ are given in Fig. 1. Equilibrium points exist at nullcline crossings. A positive slope for the horizontal nullcline indicates an unstable equilibrium point. The type —saddle or node— can be deduced from the relative locations of equilibrium points and the phase plane vector field. All three equilibrium points for the three angles of attack are unstable.

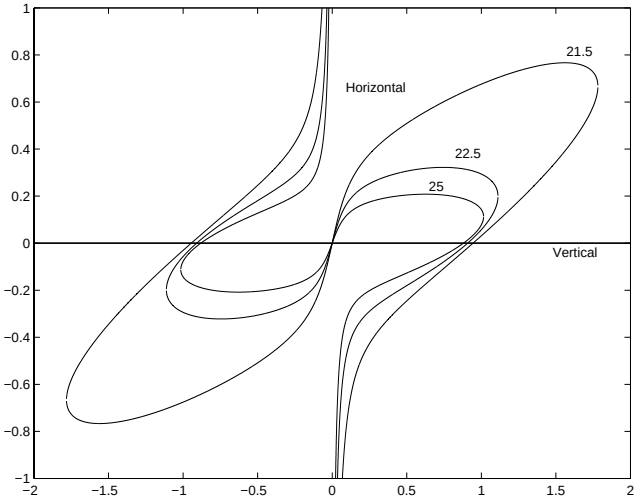

Fig. 1 Nullclines for $\theta = \{21.5, 22.5 \text{ and } 25^\circ\}$

The nullclines for $\theta = 15^\circ$ are given in Fig. 2. This angle of attack only has one equilibrium point —the origin— and that equilibrium point is stable.

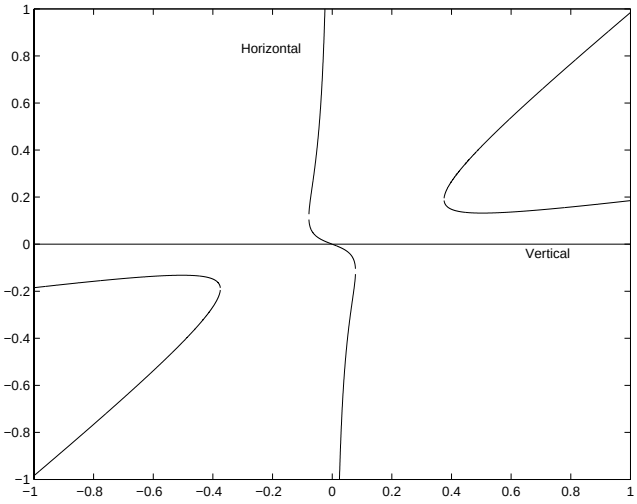

Fig. 2 Nullclines for $\theta = 15^\circ$

Nullcline analysis has characterized the phase plane without solving any differential equations. Nullclines show both trajectory behavior and equilibrium points.

Linearization

This section linearizes the equations of motion. The nonlinear state space representation is given in Eq. (5). The objective is to express the system as a linear system. The following linear system form is used:

$$\dot{x} = Ax + Bu$$

The A matrix is determined by computing the Jacobian — $\partial f_i/\partial x_j$ at x_0— for each state variable. For the delta wing model, the Jacobian is:

$$J = \begin{bmatrix} 0 & 1 \\ Q(a_1 + 3a_3x_1^2 + 2a_4x_1x_2 + a_5x_2^2) & Q(a_2 + a_4x_1^2 + 2a_5x_1x_2) \end{bmatrix}$$

The equivalent linear system at the origin is the most desirable. The equilibrium points at $x_1 \approx \pm 0.88$ correspond

to saddle points. The behavior around the saddle points is usually not particularly critical. Substituting in the origin's state vector yields the following plant matrix:

$$A = \begin{bmatrix} 0 & 1 \\ Qa_1 & Qa_2 \end{bmatrix}$$

The eigenvalues are:

$$\lambda_{1,2} = Qa_2/2 \pm 1/2\sqrt{Q^2a_2^2 + 4Qa_1}$$

The eigenvalues are given for each pitch angle θ in Table 2. The system is stable for the 15 degree pitch angle but unstable for 21.5, 22.5 and 25 degrees. The oscillation frequency decreases with decreasing pitch angles.

Table 2 Linear System Eigenvalues at Four Pitch Angles

	Eigenvalues	
θ	Real	Imag
15.0	-0.0037	0.0601
21.5	0.0025	0.1220
22.5	0.0035	0.1286
25.0	0.0058	0.1417

Limit Cycle Existence

The objective of this section is to evaluate the possible locations and trajectories of possible limit cycles. The analysis methods will establish where limit cycles can and can not exist.

Poincaré Theorem

The Poincaré theorem establishes the possible limit cycle trajectories based on equilibrium points. Poincaré's theorem from Khalil[6] is:

> Inside any period orbit γ, there must be at least one equilibrium point. ... if N is the number of nodes and foci and S is the number of saddles, it must be that N-S=1.

The equilibrium points for all four pitch angles contain a node or focus at the origin. For pitch angles of $\{21.5, 22.5 \text{ and } 25^\circ\}$, saddle points exist at $x_1 = \pm\sqrt{-a_1/a_3}$. The only N contribution comes from the origin's equilibrium point. All limit cycles must enclose the origin but not the saddles. Figure 3 shows the phase plane with a conceptual possible limit cycle trajectory γ. For harmonic

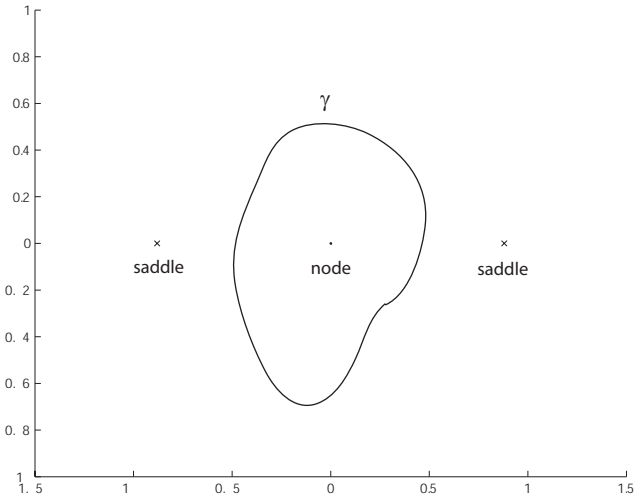

Fig. 3 Poincaré Theorem: Nodes and Saddles

and *mostly* circular limit cycles, the amplitude must be less than than the x location of the saddle points. Effectively, any possible limit cycle is restricted to $|x_1| < \sqrt{-a_1/a_3}$.

Bendixson Theorem

The Bendixson Theorem tests for the existence of limit cycles within a region of the phase plane. The Bendixson Theorem from Khalil[6] is:

> If, on a simply connected region D of the plane, the expression $\partial f_1/\partial x_1 + \partial f_2/\partial x_2$ is not identically zero and does not change sign, then the system has no periodic orbits lying entirely in D.

The Bendixson theorem is applied to the delta wing governing equation Eq. (5) to rule out phase plane regions where limit cycles are not possible. Computing the partials and substituting into the Bendixson test yields:

$$B = 0 + a_2 + a_4x_1^2 + 2a_5x_1x_2$$

The objective is to determine phase plane locations where the sign of B changes. Setting B equal to zero and solving for x_2 gives the following:

$$x_2 = \frac{-a_2 - a_4x_1^2}{2a_5x_1}$$

Figure 4 shows the $B = 0$ graphs for two angles of attack (15 and 25 degrees). The curves represent the $B = 0$ locations; any limit cycle must cross the curves. The 15 degree

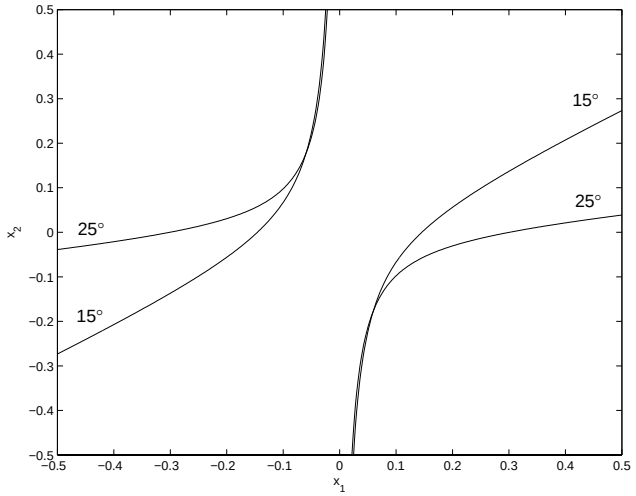

Fig. 4 Bendixson Existence

angle of attack curve is more restrictive than the 25 degree curve. Interestingly, extrapolating the Bendixson theorem indicates that the a_2 term dictates the lack of a limit cycle for smaller amplitudes. Assuming that the system doesn't have an amplitude jump —the bifurcation is smooth— indicates that the stable limit cycle bifurcation occurs when the a_2 term is zero.

Poincaré-Bendixson Theorem

The Poincaré-Bendixson theorem provides definite limit cycle existence information. The Poincaré-Bendixson Theorem from Khalil[6] is:

> ... let M be a closed bounded subset of the plane. If M contains no stable equilibrium points and if every trajectory starting in M stays in M for all future time, then M contains a periodic orbit.

The process of applying this theorem consists of finding a region of attraction. At a pitch angle θ of 25°, an unstable equilibrium point exists at the origin. Figure 5 shows trajectories that remain inside a region M for all time. Thus, the trajectories inside M are either limit cycles or going toward a limit cycle. A limit cycle exists for $\theta = 25^\circ$.

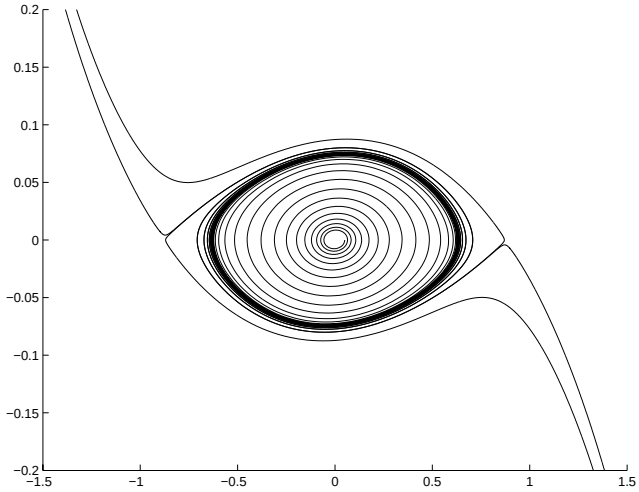

Fig. 5 Phase Plane Region of Attraction $\theta = 25°$

Phase Plane

The objective of this section is to evaluate the system dynamics and properties in the phase plane. The phase plane is established as a plot of the state vector. Roll angle, x_1, is plotted on the x axis; the roll rate, x_2, is plotted on the y axis.

Pitch Angle of 25 degrees

The system a pitch angle of 25 degrees contains an unstable origin but a stable limit cycle. The vector field is given in Fig. 6. A circular structure appears around the origin. The non-harmonic form with respect to roll angle appears as a diverging vector field for large magnitudes of roll angle. For small roll angles magnitudes between the saddle points, the model appears similar to the vector field of the harmonic pendulum. Clearly, the model breaks down for large roll angle magnitudes.

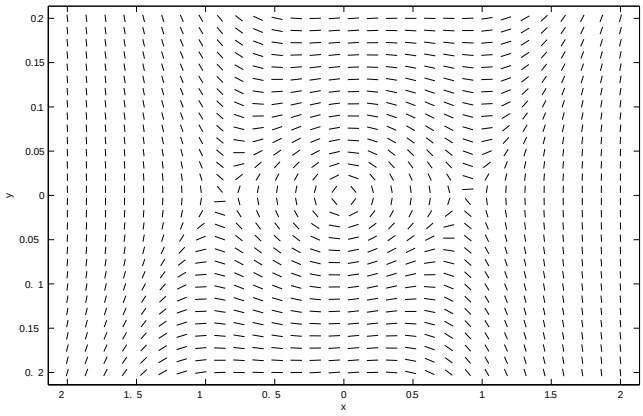

Fig. 6 Vector Field $\theta = 25°$

Typical trajectories are plotted in Fig. 7. Immediately a limit cycle is spotted with a displacement amplitude of approximately 0.6. Trajectories beginning inside the limit cycle amplitude spiral out to the limit cycle as seen in Fig. 8. At 25 degrees, the limit cycle angular frequency from Fig. 8 is 0.11 rad/s. The roll angle amplitude is 0.629.

Pitch Angle of 15 degrees

At a pitch angle of 15 degrees, the behavior has significantly changed. The origin is stable, but the limit cycle is unstable. A stable trajectory showing the stable origin is plotted in Fig. 9. The unstable behavior outside the limit cycle is shown in Fig. 10. The behavior outside the limit cycle does not match physical intuition. Again, the model appears tuned for small roll angle predictions.

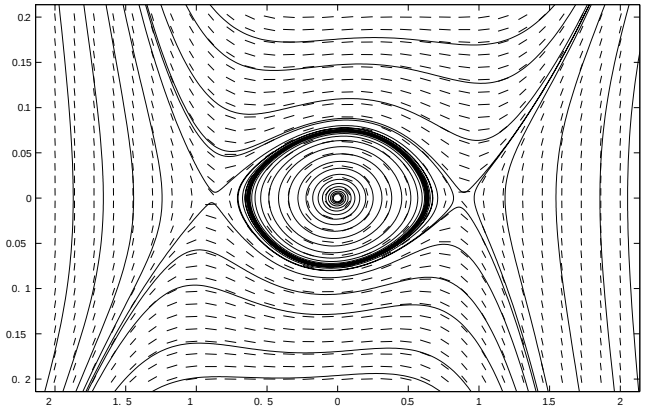

Fig. 7 Phase Plot with Trajectories $\theta = 25°$

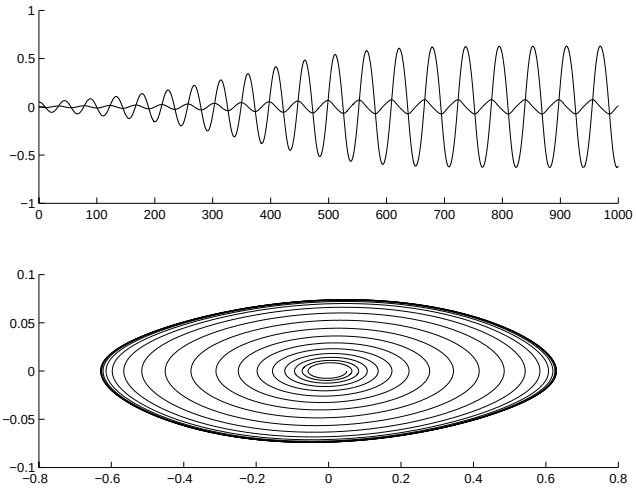

Fig. 8 Outward Trajectory at $\theta = 25°$

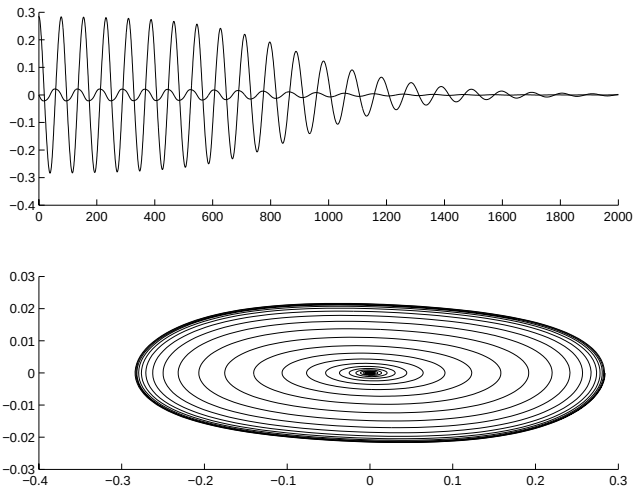

Fig. 9 Stable Trajectory Inside Limit Cycle at $\theta = 15°$

Generalization of Model Parameters

For analysis between the given pitch angles, the coefficients need to be functions of the pitch angle θ. Curves are fit to the model coefficients. The coefficient expressions are given below:

$$
\begin{aligned}
a_1 &= -0.0472\theta + 0.060 \\
a_2 &= -0.0000337\theta^2 + 0.0067\theta - 0.1143 \\
a_3 &= 0.00018\theta^3 - 0.013\theta^2 + 0.326\theta - 2.70 \\
a_4 &= -0.0022\theta^3 + 0.15\theta^2 - 3.41\theta + 25.9 \\
a_5 &= 0.0177\theta^2 - 0.48\theta + 2.32
\end{aligned}
$$

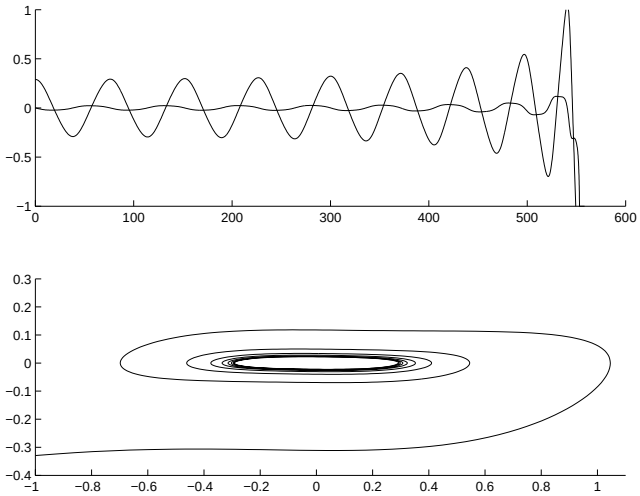

Fig. 10 Unstable Trajectory Outside Limit Cycle at $\theta = 15°$

The curve fits are reasonable within the pitch angles given as data. Extrapolated values are likely to be useless. The coefficients' jump between 15 and 21.5 degrees The a_3 and a_4 coefficients were particularly affected by this jump.

Describing Functions

Using the typical describing function approach, the motion is assumed to be sinusoidal. The nonlinear terms in Eq. (3) are expanded and higher frequency terms are dropped.

$$\begin{aligned} \phi &= a\sin\omega t \\ \phi^2\dot{\phi} &= 1/4a^3\omega\cos\omega t = 1/4a^2\dot{\phi} \\ \phi\dot{\phi}^2 &= 1/4a^3\omega^2\sin\omega t = -1/4a\ddot{\phi} \\ \phi^3 &= 3/4a^3\sin\omega t = 3/4a^3\phi \end{aligned}$$

Substituting into Eq. (3) , switching to the frequency domain and simplifying yields:

$$s^2 + Q\frac{(-a_2 - a_4 a/4)}{(1 + Qa_5/4)}s + Q\frac{\left(-a_1 - 3/4a^3a_3\right)}{(1 + Qa_5/4)} = 0$$

This form resembles the traditional second order form $s^2 + 2\omega_n\zeta s + \omega^2 = 0$. The limit cycle amplitude is approximated when the s term is zero. The limit cycle frequency is determined from the ω^2 term. Solving for the amplitude and frequency yields:

$$\begin{aligned} a &= 2\sqrt{-a_2/a_4} \\ \omega &= \sqrt{\frac{-a_1 - 6a_3\left(-a_2/a_4\right)^{3/2}}{(1/Q + a_5/4}} \end{aligned}$$

Substituting for the $\theta = 25°$ case yields:

$$\begin{aligned} a &= 0.60 \\ \omega &= 0.12 \end{aligned}$$

The describing function analysis matches the magnitude and frequency within approximately 15 percent.

Now, using the generalized model coefficients, the behavior at varied angles of attack is predicted. The limit cycle amplitude estimate is:

$$a(\theta) = 2\sqrt{\frac{-0.0000337\theta^2 - 0.0067\theta + 0.1143}{-0.0022\theta^3 + 0.15\theta^2 - 3.41\theta - 25.9}}$$

The describing function approach indicates that the amplitude depends only on the coefficients a_2 and a_4. Figure 11 shows the limit cycle amplitude versus angle of attack using the above describing function.

Both a_2 and a_4 change sign between 15 and 21.5 degrees. The sign change causes a discontinuity in the amplitude prediction. From the earlier phase plane analysis, it was seen that the 15 degree system has an unstable limit cycle. The discontinuity in the describing function estimate for amplitude appears to reflect the switch between stable and unstable behavior. Deduction suggests that the discontinuity is exactly at the origin's bifurcation point. Of course, the limiting behavior of the discontinuity is driven by whether a_2 or a_4 switches sign first. Reviewing Nayfeh, Elzebda and Mook.[4] indicates that the *wing rock* bifurcation point is approximately "19–20" degrees.

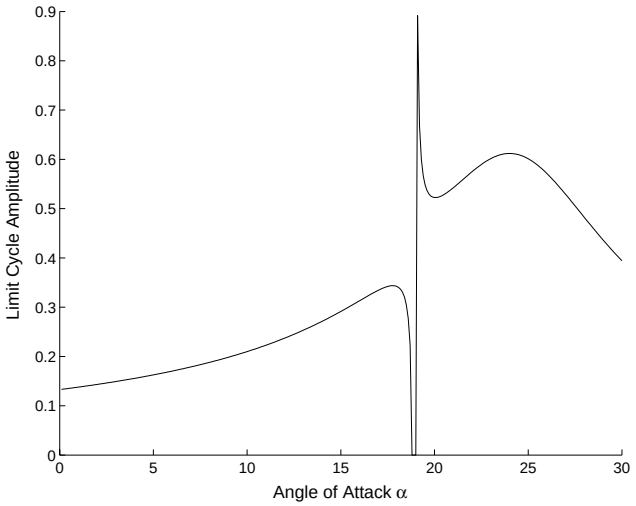

Fig. 11 Limit Cycle Amplitudes using Describing Function Analysis

The describing function approach is simple and provides good estimates primarily because the wing rock trajectories for the limit cycle are almost perfectly circular. The describing function analysis when combined with the traditional phase plane analysis gave interesting insights.

Controls Guidelines

The fundamental constraint for controls is stability. The goal is to make the system uniformly asymptotically stable in the large. The wing rock limit cycle should be removed with no exceptions. A control law that minimizes or eliminates overshoot is desired. Excessive overshoot causes piloting problems. Other constraints concern the wing's roll performance.

For control, the input is a roll moment. Control provided by ideal moment generator. No dynamics will be associated with the input to keep the system 2nd order. The governing equation for controls with an input u is:

$$\ddot{\Phi} = QL + u$$

The input roll moment will have an amplitude limitation near $u = 0.1$ to simulate the limited motion of aircraft control surfaces.

Pole Placement

Pole placement is a linear control method. The objective is to stabilize the motion at the origin. The linear system corresponding to the origin is:

$$\dot{x} = \begin{bmatrix} 0 & 1 \\ Qa_1 & Qa_2 \end{bmatrix} x + Bu$$

A control scheme of the following form is input into the control u.

$$u = \begin{bmatrix} 0 & 0 \\ K_1 & K_2 \end{bmatrix} x$$

Combining the linear system with the control scheme yields:

$$\dot{x} = \begin{bmatrix} 0 & 1 \\ Qa_1 + K_1 & Qa_2 + K_2 \end{bmatrix} x$$

The eigenvalues of this combined linear system are:

$$\lambda_{1,2} = \frac{Qa_2 + K_2}{2} \pm \frac{\sqrt{Q^2a_2^2 + 2K_2Qa_2 + K_2^2 + 4Qa_1 + 4K_1}}{2}$$

Placing the poles at -0.1 and -1.0 and solving yields gains of $K_1 = -0.08$ and $K_2 = -1.11$. The control scheme is:

$$u = -0.08x_1 - 1.11x_2$$

A schematic for the system and control scheme is given below. The phase plane with the control input is given be-

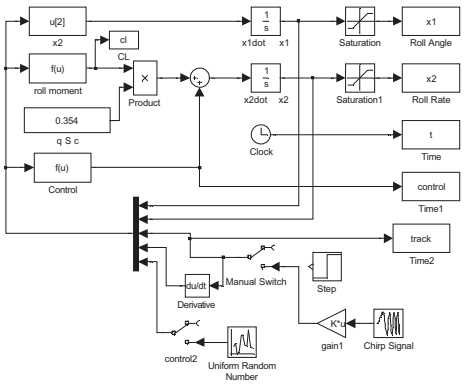

Fig. 12 Pole Placement Matlab Schematic

low. Notice that the domain of attraction is extended to

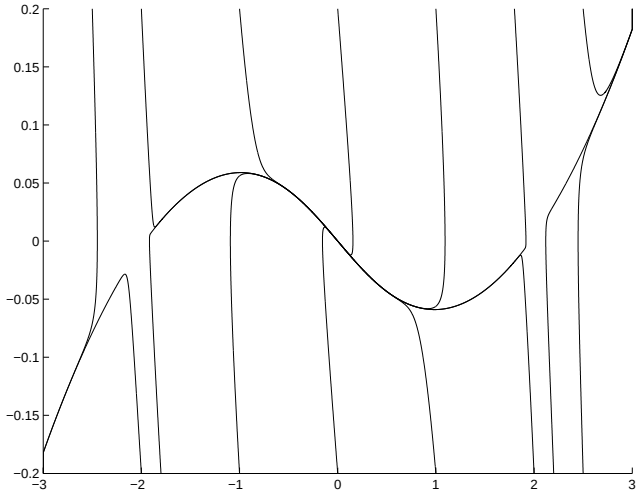

Fig. 13 Pole Placement Phase Plane Plot

almost $x_1 = \pm 2$. The trajectories appears to move along an inverted-sine-wave-like surface.

The displacement response is given in Fig. 14. Notice that the linear control scheme drives the displacement to zero for small initial displacements, but fails for large initial displacements.

Unfortunately, the linear control scheme drives the motion to the origin —an equilibrium point. For reasonable gains, the control law provides sufficient damping using x_2 to eliminate the limit cycle. As expected, control laws feeding back only displacement can eliminate the limit cycle.

Next, pole placement for a tracking problem. The tracking motion consists of a step input starting at t=20 with a displacement of 0.1. The control scheme does not track well. The displacement converges before reaching the desired

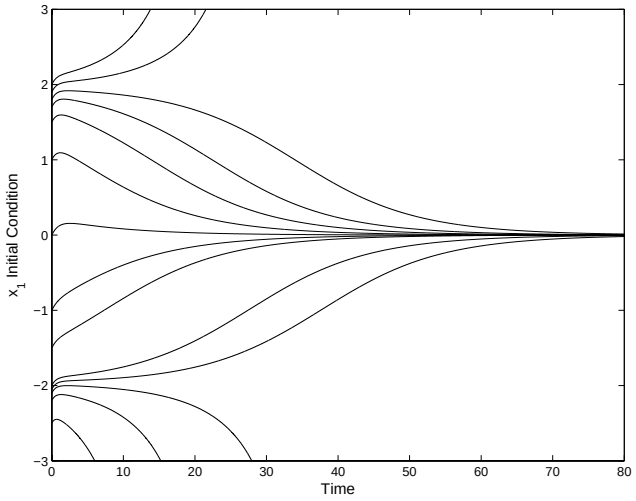

Fig. 14 Pole Placement Displacement Plot

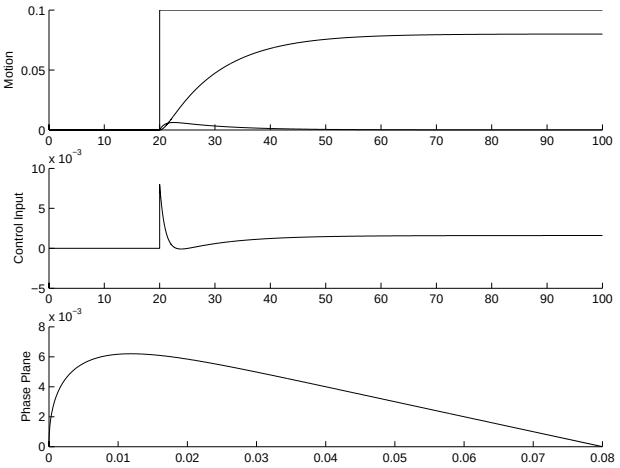

Fig. 15 Pole Placement Step Input Tracking

tracking motion. As expected, the control input converges to a non-zero value. Intuition suggests that the error will never converge to zero for these linear control laws. Adding an integral control on tracking error is a possible solution. This is a spectacular —but expected— failure!

Ricatti

The Ricatti LQR control law synthesis method creates a robust linear system control law. The required inputs are the linear system's plant matrix and two weighting matrices for the state and control vectors. Matlab solved the corresponding Ricatti equation. The state vector weighting matrix Q was selected with diagonal terms corresponding to the limit cycle amplitude. The control weighting matrix R corresponds to the maximum control power available. Using Matlab, the LQR control law is:

$$u = -0.559x_1 - 1.22x_2$$

The first evaluation testcase is the Ricatti control law with an initial displacement condition. Figure 16 shows the Ricatti control law's performance. The control law stabilizes the system with a smooth control input.

Next, the Ricatti control law is tested with noise in Fig. 17. The noise introduces a small input induced oscillation about the origin. Otherwise, the control law's performance is good.

The Ricatti control law is tested for tracking performance. A step input is shown in Fig. 18. The control law tracks excellently even with noise. This excellent performance is

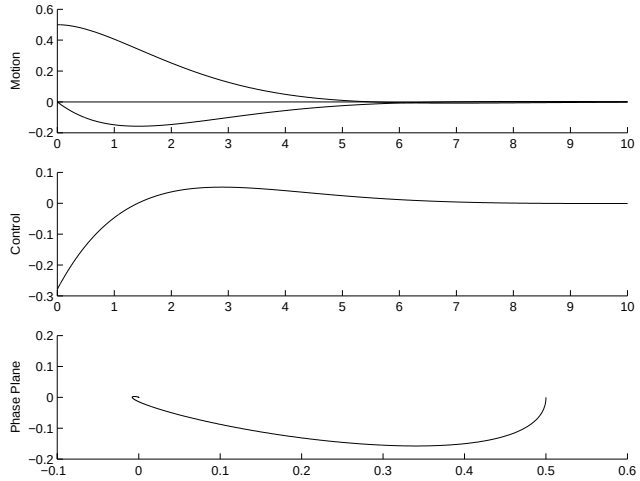

Fig. 16 Ricatti Control

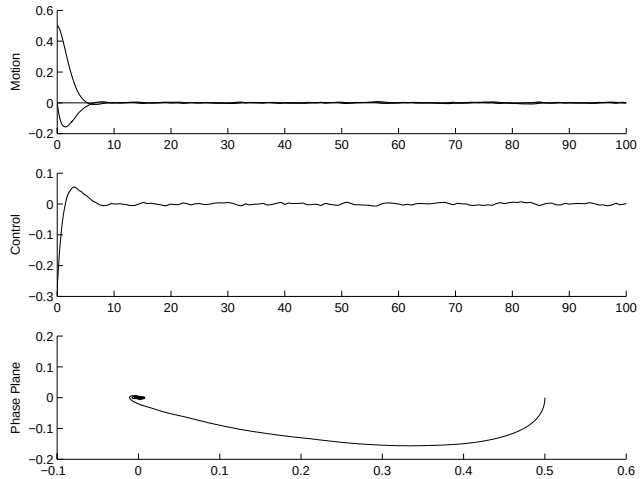

Fig. 17 Ricatti Control with Noise

surprising given both the nonlinear system and the input noise. The Ricatti control law converges to the tracking signal when the pole placement does not. This is disturbing.

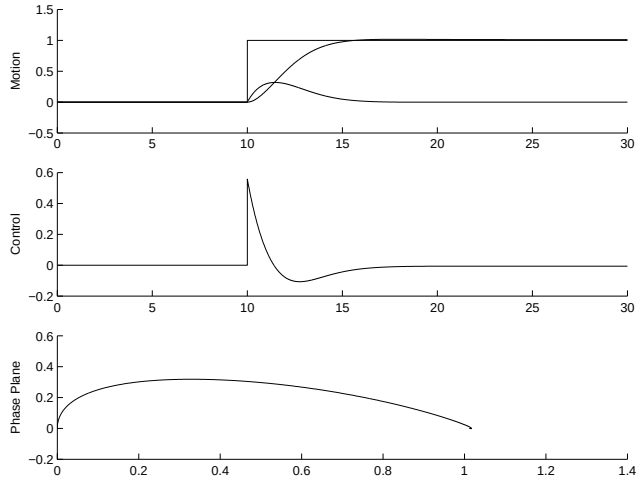

Fig. 18 Ricatti Step Tracking

Finally, the Ricatti control law is tested for tracking performance with a linear frequency swept chirp. The system response is given in Fig. 19. For this tracking problem, the Ricatti control law increasingly becomes in error as the chirp frequency increases.

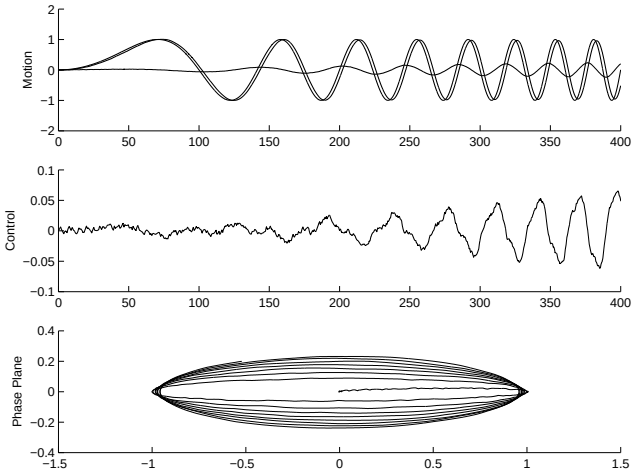

Fig. 19 Ricatti Chirp Tracking

Sliding Mode

Sliding mode control is used for stability and tracking control of the delta wing model. The state space representation is repeated below with unknown noise w added. A scalar b is pre-multiplies the control input.

$$\begin{aligned} \dot{x}_1 &= x_2 \\ \dot{x}_2 &= QC_L + bu + w \end{aligned}$$

For later robustness, nominal models are used.

Control Law Derivation

Tracking is established with a tracking vector, $\tilde{x}$ as the difference between the state vector, x, and the desired motion, x_d.

$$\tilde{x} = x - x_d$$

Select a sliding surface S.

$$S = \dot{\tilde{x}} + \lambda\tilde{x} = (\dot{x} - \dot{x}_d) + \lambda(x - x_d)$$

Ensure the resulting system is Lyapunov stable by introducing a sign(S) function. For the Lyapunov function $V = 1/2S^2$, $\dot{V}$ is negative —and the system is stable— with the following:

$$\dot{V} = S\dot{S} = -\eta|S|$$

This reduces to

$$\dot{S} = \ddot{x} - \ddot{x}_d + \lambda(\dot{x} - \dot{x}_d) = -K\text{sign}(S)$$

Rearranging the terms yields:

$$QC_L + \hat{b}u - \ddot{x}_d + \lambda(\dot{x} - \dot{x}_d) + K\text{sign}(S)$$

Solving for the control u yields the following:

$$u = -\frac{1}{\hat{b}}\left(QC_L - \ddot{x}_d + \lambda\dot{x} - \lambda\dot{x}_d + K\text{sign}(S)\right)$$

The wing rock angular frequency is approximately 0.1 radian per second. This is a period of 50. A sliding time constant of 10 was chosen. $\lambda = 1/10 = 0.1$. The reaching time constant of 5 gives $\eta = 0.06$.

The robustness is assured through the selection of a *large enough* gain K. The primary difficulty is establishing the magnitudes of C_L. The difficulty concerns the maximum values of the state vectors. Evaluating the absolute magnitude $|C_L|$ at x_1=1.5 and $x_2 = 0.2$ yields $C_L \approx 0.2$. Also, a harmonic trajectory was created at the maximum expected values of the state vectors. This simulation approach gave a maximum $C_L \approx 0.2$. The noise input is bounded by $|w| \leq 0.02$. The control input is assumed to be bounded by $b_{max} = 1.1$ and $b_{min} = 0.8$ so that $\beta = 1.17$. For robustness, the gain K is:

$$K \geq \beta(|w| + \eta) + (\beta - 1)|C_L| \approx 0.11$$

Sliding Mode Results

The sliding mode control was implemented in Matlab. The schematic is shown in Fig. 20.

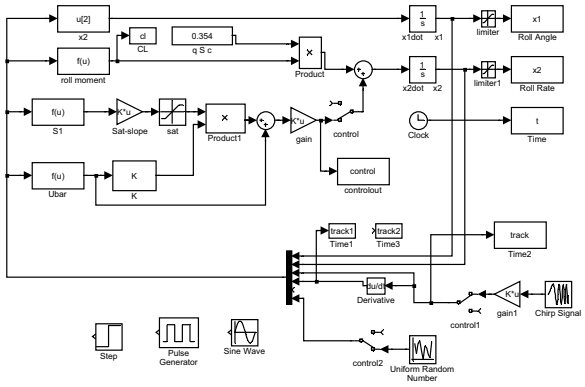

Fig. 20 Sliding Mode Control: Matlab Schematic

The initial simple testcase is used to establish the stability performance of the control law. Figure 21 shows the system response to an initial displacement of 1 unit. This initial condition is outside the limit cycle's domain of attraction. The

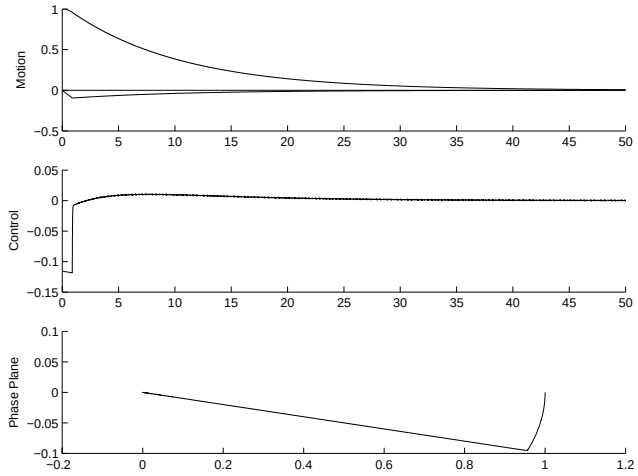

Fig. 21 Sliding Mode: Stability Performance

sliding mode control works as expected. The initial reaching phase occurs within about 1 non-dimensional second. The sliding phase requires approximately 25 seconds to reach 90 percent of the steady state displacement. The phase plane plot in Fig. 21 shows both the reaching and sliding portions of the stabilization.

The next testcase evaluates the stability performance with the presence of noise. Random noise with maximum amplitude of 0.02 is input directly into the C_L moment. Figure 22 shows the system response to an initial displacement of 1 unit with noise. Again, the sliding mode control provides excellent stabilization.

The next testcase evaluates the tracking ability of the control law. Two tracking signals are tested. First, a step tracking signal is shown in Fig. 23. The step intrinsically contains infinite derivatives, so the control law attempts to provide as much control power as possible. Otherwise, the tracking performance is good. Again, the motion follows the sliding surface as seen in the phase plane plot. Tracking with noise is shown in Fig. 24. Again, the control system tracks to the desired signal.

Second, a frequency swept chirp is shown in Fig. 25. The desired track and the actual system response lie almost together. The actual system is slightly out of phase with the desired signal, but otherwise the tracking is excellent. Interestingly, the chirp displacement is 1.0. This is almost

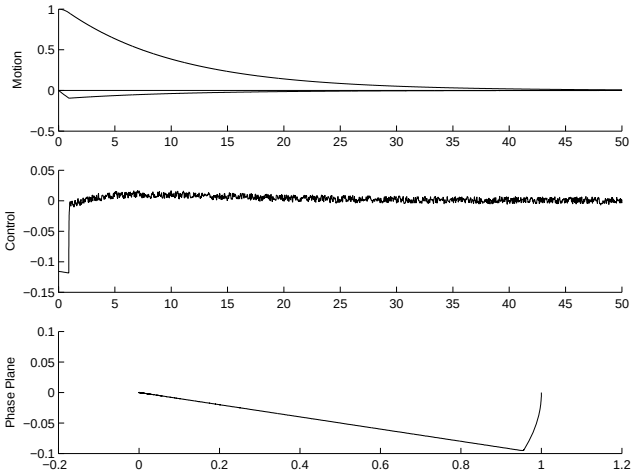

Fig. 22 Sliding Mode: Stability Performance with Noise

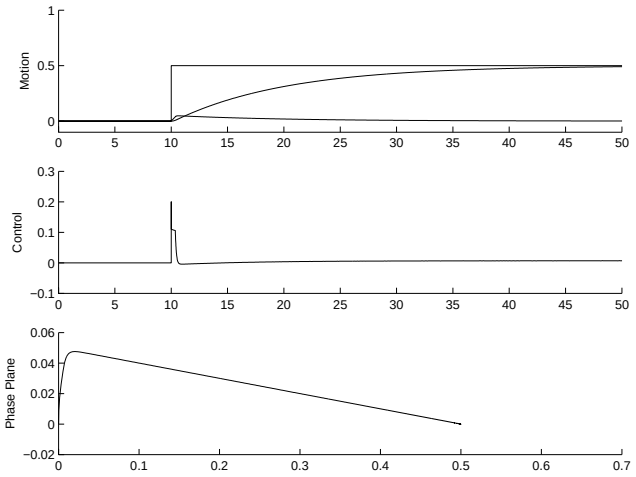

Fig. 23 Sliding Mode: Step Tracking Performance

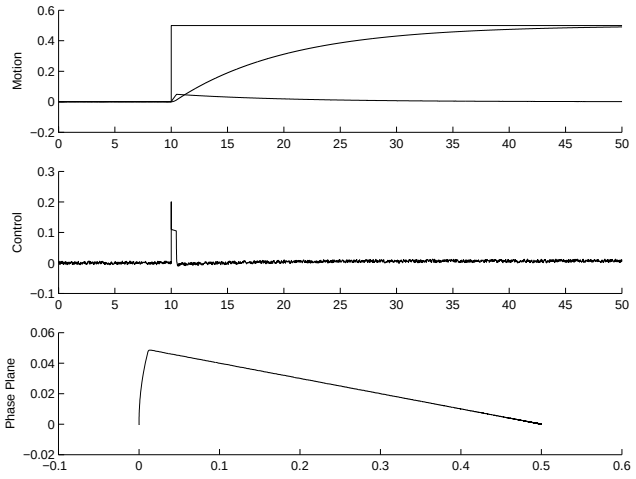

Fig. 24 Sliding Mode: Step Tracking Performance with Noise

twice the limit cycle's amplitude. Chirp tracking with noise is shown in Fig. 26. Again, the sliding mode control tracks the desired signal nicely.

For comparison, Fig. 27 shows the controls-off system with noise starting from the origin. The noise magnitude was decreased to 0.005, otherwise the system exits the limit cycle region and diverges. When the noise level remains at 0.02, the system goes unstable within 2 actual seconds. The sliding mode control allows the system to track a desired signal well outside the open-loop stability region with 4 times more

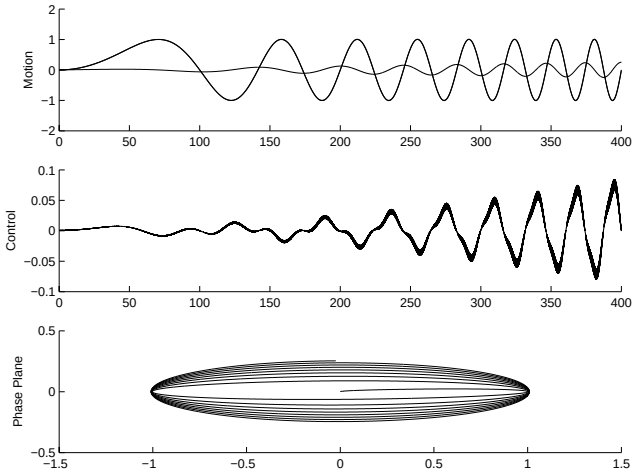

Fig. 25 Sliding Mode: Chirp Tracking Performance

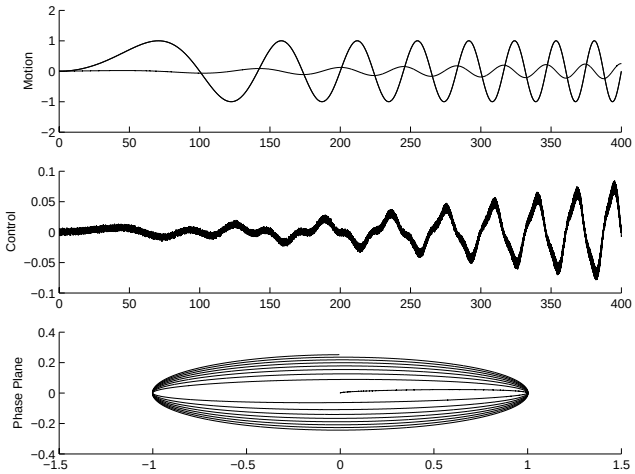

Fig. 26 Sliding Mode: Chirp Tracking Performance with Noise

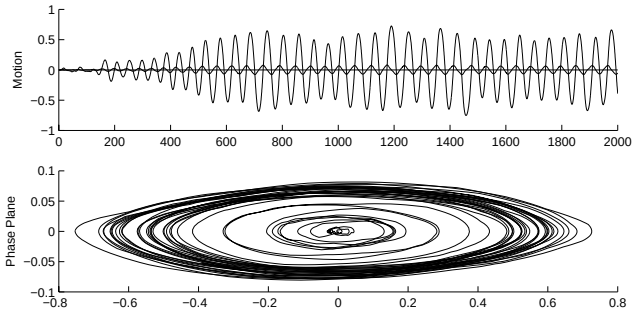

Fig. 27 Open Loop with Noise

noise than allowed for passive stability.

Control Lyapunov Function

The objective is to design a control law that automatically satisfies a candidate Lyapunov function. The state space representation of the equations of motion are:

$$\begin{aligned} \dot{x}_1 &= x_2 \\ \dot{x}_2 &= Q\left(a_1 x_1 + a_2 x_2 + a_3 x_1^3 + a_4 x_1^2 x_2 + a_5 x_1 x_2^2\right) + Qu \end{aligned}$$

Concentrate on $\dot{x}_2$ and evaluate the individual terms for their contribution to stability. Assume that the angle of attack is over 15 degrees which gives consistent coefficient signs for a_i.

$$|a_1| < 0, \quad |a_2| > 0, \quad |a_3| > 0, \quad |a_4| < 0, \quad |a_5| > 0$$

Evaluate individual terms to establish if the term is stable or unstable. The objective is to keep the stable terms and cancel only the unstable terms. x_1 and x_1^3 terms correspond to restoring forces and are stabilizing if negative. x_2 terms correspond to damping forces and are stabilizing if negative. The $x_1^2 x_2$ term is tricky. However, x_1^2 is always positive, so the term acts as a nonlinear damping. Again, a negative term is stabilizing. For the same reasons, $x_1 x_2^2$ is stabilizing with a negative term.

$$\dot{x}_2/Q = \underbrace{a_1 x_1}_{\text{good}} + \underbrace{a_2 x_2}_{\text{bad}} + \underbrace{a_3 x_1^3}_{\text{bad}} + \underbrace{a_4 x_1^2 x_2}_{\text{good}} + \underbrace{a_5 x_1 x_2^2}_{\text{bad}} + u$$

The objective is to synthesize a control law that cancels the *bad* terms. Further inspection shows that the resulting system —including the new control law— has no explicit linear damping term from x_2. Adding this damping term yields the following control law:

$$u = -\left(a_2 x_2 + a_3 x_1^3 + a_5 x_1 x_2^2\right) - \zeta x_2$$

The combined system with the control law is:

$$\begin{aligned} \dot{x}_1 &= x_2 \\ \dot{x}_2 &= Q\left(a_1 x_1 + a_4 x_1^2 x_2 - \zeta x_2\right) \end{aligned}$$

From inspection with a simple Lyapunov Function ($V = 1/2x_1^2 + 1/2x_2^2$), the new system is UASIL. The critical assumption for stability concerns the control power available. The control law depends on the cube of roll angle. Large unwanted roll angles will require large control inputs.

The CLF control law is implemented in Matlab as given in Fig. 28. The overall control law is simple and easy to implement.

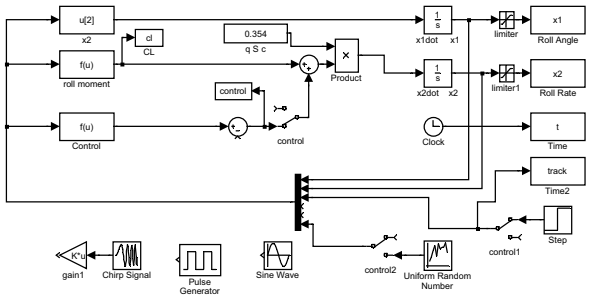

Fig. 28 CLF Schematic

The first test contains a clean input —no noise— with an initial condition followed by step input. The initial condition tests the stabilization performance. The step input tests the tracking performance. Figure 29 gives the system response. The control law stabilizes the system to the origin but does not converge to the tracking signal. The problem occurs for the same reason the linear control scheme failed to converge to a tracking signal.

The second test is a noisy roll moment with an initial condition followed by a tracking step. The noise has a maximum magnitude of 0.02. Again, the control law converges the system to the origin but does not provide good tracking.

Including a simple integral control should assist with convergence to the tracking inputs. However, larger tracking inputs cause unstable oscillations from the overshooting integral control. The actual tracking response for this control law remains poor even with adding integral control.

Conclusions

Delta wing aerodynamics are complicated. The objective of this project was to analyze and control a simple analytical roll model.

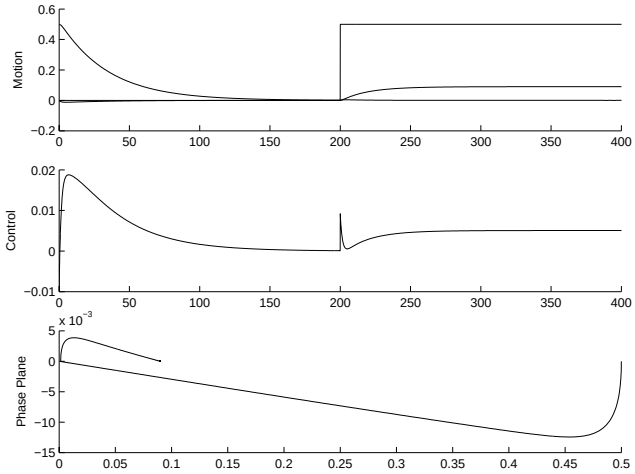

Fig. 29 CLF Tracking

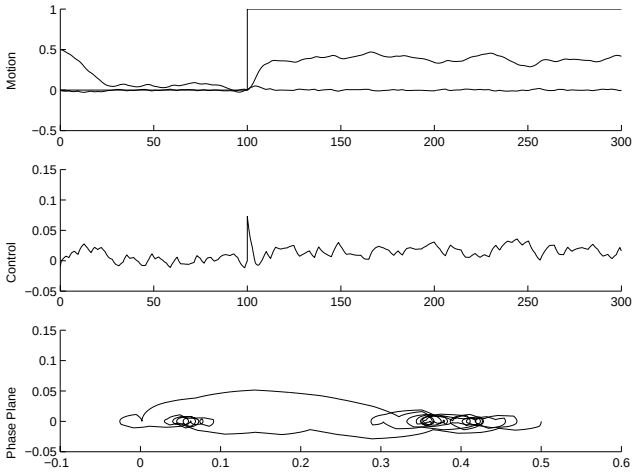

Fig. 30 CLF Tracking with Noise

The first difficulty is finding a *good* system model for the aerodynamics. Comparison between a physically consistent roll moment model and the selected model indicates possible restrictions on the selected model's operating range.

The traditional phase plane analysis techniques and existence methods indicated the overall system properties without solving the second order differential equation for roll. The phase plane plots showed the entire system behavior in a particular region.

The describing function approach for finding limit cycle amplitudes and frequencies gave accurate predictions. The limit cycles were almost perfectly circular, so the describing function approach works well for this particular problem.

Linear control laws allowed for good stabilization but not good tracking. The linear control laws give smooth control inputs unlike the nonlinear control laws. Nonlinear control laws gave good stabilization and tracking performance. In particular, the sliding model control allowed for robust performance.

References

[1]Nelson, R. C., *Flight Stability and Automatic Control*, McGraw-Hill, 2nd ed., 1998.

[2]Arena, A. S., *An Experimental and Computational Investigation of Slender Wings Undergoing Wing Rock*, Ph.D. thesis, University of Notre Dame, Notre Dame, Indiana, April 1992.

[3]Ericsson, L. E., "Wing Rock Analysis of Slender Delta Wings, Review and Extension," *Journal of Aircraft*, Vol. 32, No. 6, November-December 1995, pp. 1221–1226.

[4]Elzebda, J. M., Nayfeh, A. H., and Mook, D. T., "Analytical Study of the Subsoic Wing-Rock Phenomenon for Slender Delta Wings," *Journal of Aircraft*, Vol. 26, No. 9, September 1989, pp. 805–809.

[5]Go, T. H. and Ramnath, R. V., "Analysis of the Two-Degree-of-Freedom Wing Rock in Advanced Aircraft," *Journal of Guidance, Control, and Dynamics*, Vol. 25, No. 2, March–April 2002, pp. 324–333.

[6]Khalil, H. K., *Nonlinear Systems*, Prentice Hall, New Jersey, 3rd ed., 2002.